

# Effect of process parameters of micro-plasma arc welding on morphology and quality in stainless steel edge joint welds

K. H. Tseng, S. T. Hsieh and C. C. Tseng

The effects of the process parameters of micro-plasma arc welding (micro-PAW) on the morphology and quality of stainless steel edge joint welds were investigated. Micro-PAW was applied on type 304 stainless steels to produce an edge joint weld. Welding experiments were carried out for various combinations of arc current, welding speed, arc length, shielding gas, and clamp distance, with all other operating conditions held constant. The experimental results indicated that the collimated shape of the low current plasma arc was mainly responsible for the low sensitivity of the weld morphology to variations in the nozzle standoff distances. The arc voltage increased with increasing quantity of added hydrogen in the argon shielding gas. It was also found that satisfactory edge joint welds can be formed using a clamp distance of 0.35 mm, and that the edge joint penetration on a 0.1 mm thickness stainless steel is about 60% of the clamp distance. STWJ1373

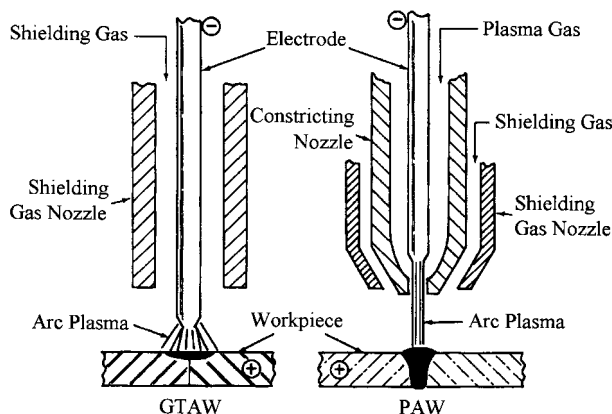
The authors are in the Welding Technology Section, Metal Processing Research and Development Department, Metal Industries Research and Development Centre, 1001 Kaonan Highway, Nantzu, Kaohsiung, Taiwan 811, Republic of China (khtseng@mail.mirdec.org.tw). Manuscript received 18 November 2002; accepted 4 February 2003.

© 2003 IoM Communications Ltd. Published by Maney for the Institute of Materials, Minerals and Mining.

## INTRODUCTION

Fabrication of metal structures in space will require extensive use of various metal joining processes. The plasma arc welding (PAW) process is one of several methods being considered for this purpose. Plasma arc welding is an arc welding process in which coalescence, or the joining of metals, is produced by heating with a constricted arc between a non-consumable electrode and the workpiece (transferred arc) or the electrode and the constricting nozzle (non-transferred arc).<sup>1-3</sup> The PAW process is essentially similar in operation to the gas tungsten arc welding (GTAW) process in that the arc is used as a heat source to fuse the joint and, when required, filler metal is added to form the welds. In contrast to the GTAW process, because the electrode is recessed within the constricting nozzle (Fig. 1), the PAW process has several singular operating characteristics as follows.<sup>4-7</sup>

(i) A pilot arc can be formed between the electrode and the constricting nozzle; since a pilot arc is relatively inefficient as a heat source, an arc must be transferred from the nozzle to the workpiece to be



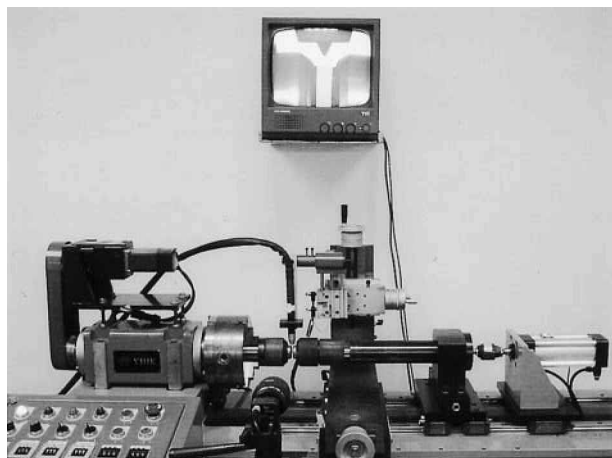
## 1 Comparison of gas tungsten arc welding (GTAW) and plasma arc welding (PAW) processes

welded to enable heat to be generated in forming the arc roots.

- (ii) The nozzle constricts the plasma to form a columnar arc which, compared with the gas tungsten arc, is more directional and exhibits a lack of puddle size sensitivity to arc length changes.
- (iii) Controlled penetration is achieved via the use of a keyhole mode welding technique. The most significant difference between the GTAW and plasma welding arcs lies in the keyhole technique. This technique produces a small hole that is carried along the weld bead. During the welding process, the hole progressively cuts completely through the workpiece, with the molten weld pool flowing behind to form the weld under surface tension forces.
- (iv) Since the electrode is held within the constricting nozzle, it is not possible for the electrode to touch the weld pool. The possibility of tungsten inclusions in the weld metal is reduced and the period between electrode adjustments is extended.

The PAW technique can offer higher quality welds than GTAW and at lower equipment cost than laser beam or electron beam welding, and it may be the most effective process for many applications. These include the welding of stainless steel expandable bellows, where PAW is more tolerant to joint misalignment than laser beam welding and gives better weld penetration than the GTAW technique. Consequently, the practical PAW process is widely accepted in the aerospace, chemical, naval and shipyards, and nuclear industries, etc.

Many instruments require welds of great accuracy. The micro-plasma arc welding (micro-PAW) process, with its extremely fine control and high precision, provides the only



## 2 Micro-PAW equipment used

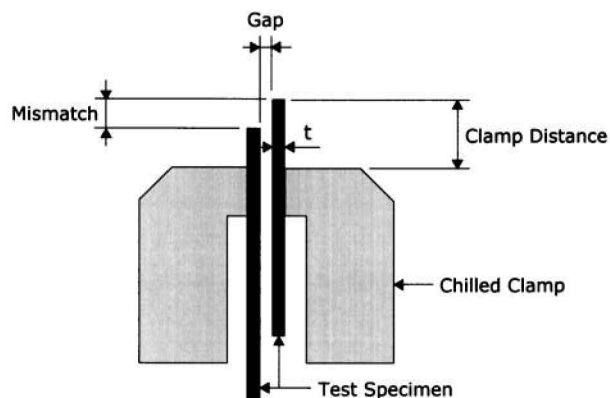
viable practical possibility of producing such critical welds. Micro-PAW technology was developed to obtain a very stable, controllable arc for joining fine sheet down to 0.1 mm thickness, and wire and mesh sections, because of the precise control that is achievable in respect of arc initiation and input of heat to the work-piece. Typical applications of micro-PAW include joining of aspiration needles, battery seals, catheter guide wires, diaphragm bellows, enclosure filters, microrelay cases, etc.

A needle plasma jet is obtained by passing a very low current arc through a small diameter orifice.<sup>7,8</sup> The narrow needlelike stiff arc generated at currents within the range 0.1 to 15 A can prevent arc wander; the equivalent gas tungsten arc at comparable current suffers from instabilities because of arc wander, and is much more diffuse. Compared with a gas tungsten arc, the micro-plasma jet has improved low current arc direction and stiffness, increased arc stability, and greatly reduced sensitivity to changes in arc length. It is possible to vary the arc length over a comparatively wide range (up to 20 mm) without adversely affecting stability and, owing to the nature of the constricted plasma, without causing excessive spreading of the arc.<sup>4</sup>

The successful joining of foil thickness metal sheets using the micro-PAW technique depends on the availability of all necessary equipment (power source, cooling unit, torch, plasma gas, and shielding gas), precise control systems (orientation and motion), adequate joint design and fixturing, and careful cleaning procedures. The process characteristics and the operating parameters, which can influence weld morphology and quality, become rather significant in such low current foil welding applications. In the present work, detailed experiments were conducted to investigate the effect of micro-PAW process parameters on morphology and quality in stainless steel edge joint welds.

## EXPERIMENTAL

Austenitic stainless steel 304 having the chemical composition and mechanical properties given in Table 1 was used. The equipment used in the present work is shown in Fig. 2.



Joint type	Gap	Mismatch	Clamp distance
Edge-joint	0.5t max.	1t max.	2~4t

## 3 Joint design and fixturing tolerances on 0.1 mm thickness stainless steel

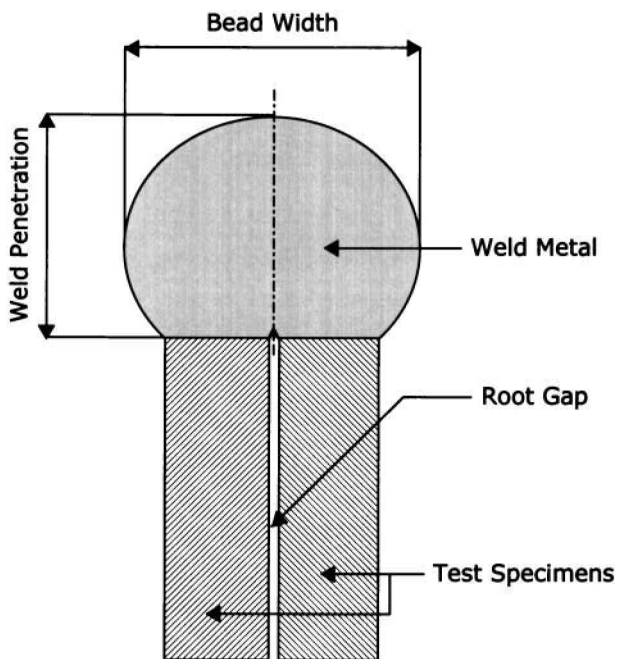
Micro-PAW was carried out with 31.5 mm outer diameter, 0.1 mm thickness test specimens using the melt in welding mode. The programmable and transistorised direct current power source, supplying a regulated arc current of 0.08 to 50 A, was used to generate a low current needlelike arc on negative polarity. A machine mounted welding torch having a standard 1.5% lanthanated tungsten electrode (1 mm diameter) was used. The electrode tip configuration was a sharp point with a 30° included angle. The preferred plasma gas for low current plasma welding is argon because its low ionisation potential ensures reliable starting and a dependable pilot arc. In the present work, the orifice gas flowrate was 0.25 L min<sup>-1</sup> through a 0.8 mm diameter orifice and pilot arc current was fixed at 5 A. Argon is also a suitable shielding gas for welding stainless steels, but it does not necessarily produce optimum joining results. The welding processes were performed using pure argon and Ar-H<sub>2</sub> mixed gases. The shielding gas flowrate was 7 L min<sup>-1</sup> for all compositions.

To achieve uniform fusion in thin sheet material, it is crucial that the component edges are accurately machined and that the clamping provides a uniform heat sink. The joint design and fixturing tolerances in the present work are shown in Fig. 3. For a high precision edge joint on 0.1 mm thickness stainless steel, a maximum joint gap of 0.05 mm is permitted. The maximum allowable joint mismatch is 0.1 mm to ensure that both joint edges are in continuous contact and that both edges melt simultaneously to fuse together into a smooth fusion weld. Additionally, clamp distances of 2 to 4 times the thickness of the sheet are required to ensure correct joint fitup and prevent warping of the joint edges. The chilled clamps that held test specimens in contact were manufactured from brass to prevent heat buildup.

Strict attention to the initial cleaning of the component surfaces is necessary because oxides or grease films affect the surface tension of melted joint edges and the degree of melting attained at a given heat input level when thin metals are welded. Cleaning of the grease films was necessary to prevent the formation of porosity. With respect to cleaning,

**Table 1 Chemical composition (wt-%) and mechanical properties of type 304 stainless steel used**

C	Si	Mn	P	S	Cr	Ni	Fe	Yield strength, MPa	Elastic modulus, MPa	Poisson's ratio
0.07	0.47	1.12	0.02	0.03	18.5	8.25	Bal.	287	191	0.25



4 Schematic illustration of weld bead geometry of edge joint

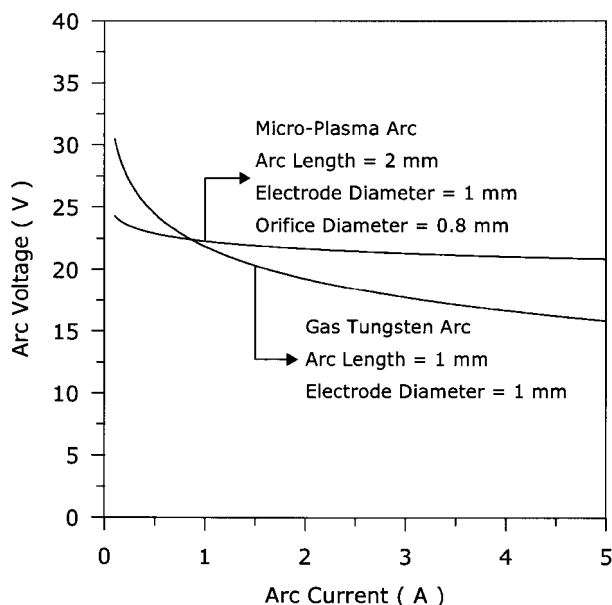
the number of defects can be kept low using an ultrasonic method. Before welding, all test specimens in the present work were cleaned using a conventional ultrasonic cleaner with acetone solvent to remove surface impurities, and the cleaned parts were stored in plastic bags until ready for welding.

Figure 4 shows a schematic illustration of the weld bead geometry. Optical microscopy was used to measure the bead width and weld penetration. A minimum of three measurements were made and the average values are reported. All metallographic specimens were prepared by mechanical lapping, grinding, and polishing to 0.3 μm finish.

**RESULTS AND DISCUSSION**

**Static volt–ampere characteristic of low current arc welding process**

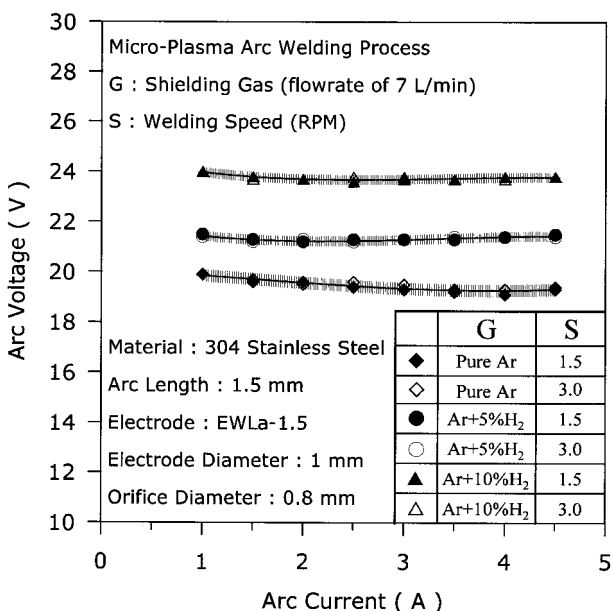
The relationship between arc voltage and arc current at a certain arc length is known as the static volt–ampere characteristic. The gas tungsten arc and plasma arc static volt–ampere characteristics are compared in Fig. 5 for arc currents below 5 A in argon shielding gas. The voltage of an argon shielded tungsten arc increases from 15 to 23 V, a change of about 53%, as the arc current is reduced from 5 to 1 A. It can be seen that the negative slope of the gas tungsten arc volt–ampere characteristic curve is fairly steep at extremely low current. In a low current PAW process, the slope of this volt–ampere characteristic curve is almost flat, with the arc voltage increasing from 21 to 22 V, i.e. a 5% change, as the arc current is again reduced from 5 to 1 A. In contrast to the GTAW process, the PAW process combines a continuously operating pilot arc within the torch and arc constriction to provide a needlelike plasma jet, which is continuous and stable at very low currents. It thus provides greater arc stability than a gas tungsten arc. To reiterate, in the present work a needle plasma arc welding technique was developed to provide an arc that is stable at very low currents for melt in welding of thin gauge metals.



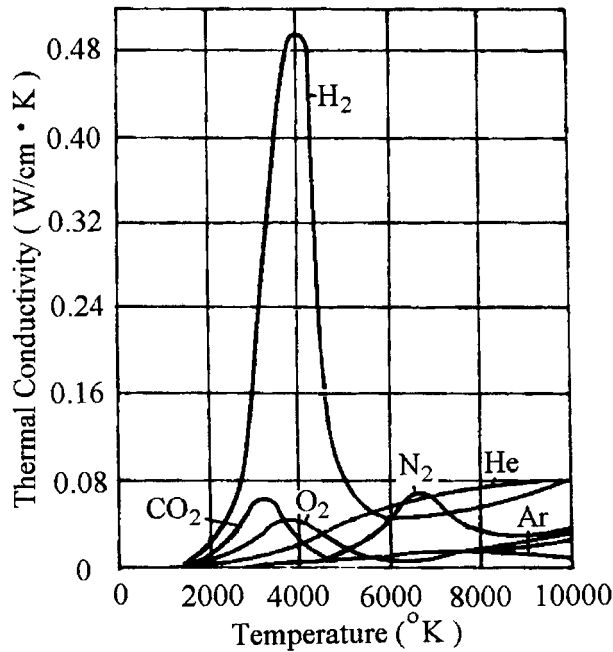
5 Comparison of gas tungsten arc and micro-plasma arc static volt–ampere characteristic curves

**Effect of hydrogen in argon shielding gas on arc characteristic and weld morphology**

Generally, arc power equals the heat lost from the plasma arc column, and the arc characteristic is a function of the heat loss.<sup>9</sup> Figure 6 shows the characteristics of the plasma arc in the micro-PAW process for various amounts of added hydrogen in the argon shielding gas at a certain arc length. The arc current was maintained at a constant value, and it was found that the arc voltage increases as the amount of hydrogen added to the argon atmosphere increases. Figure 7 shows the thermal conductivity of each of the gases. The diagram shows that the thermal conductivity of hydrogen is much higher than that of argon at operating temperatures typical of the welding arc because of the dissociation and recombination effects. Consequently, more heat is lost from the plasma arc column



6 Arc characteristics for various shielding atmospheres



7 Thermal conductivity of possible shielding gases as function of temperature (after Ref. 10)

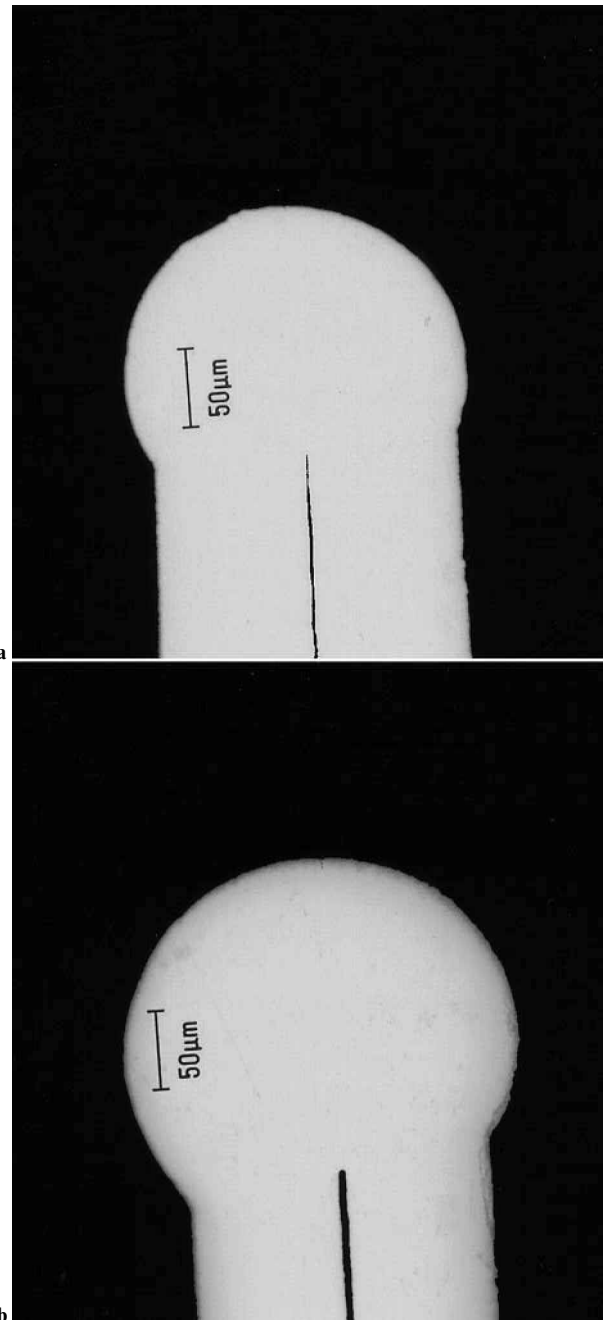
as hydrogen is added to the argon shielding gas. The loss of energy must be balanced by the gas in the plasma arc column; the power generated in the arc, the product of arc current and arc voltage, is therefore also increased. These effects increase the arc voltage at a given arc current as hydrogen is added to the pure argon atmosphere.

The composition of the shielding mixture for arc welding depends primarily on the type of base metal to be welded. Notably, for high alloy stainless steels, the use of shielding mixtures consisting of argon and about 1–5% added hydrogen is preferred, with the risk of porosity in the welds occurring at greater hydrogen contents.<sup>8,11,12</sup> Figure 8 shows the macroscopic sections of solidified welds obtained using the micro-PAW process with various shielding mixtures at a constant arc current. The arc voltages varied owing to the different shielding gases used. As hydrogen is added to the pure argon atmosphere, increasing the arc voltage and consequently the arc power, the arc heats up and heat transfer to the fusion zone becomes more efficient, melting a large quantity of the base metal.

It can be seen in Fig. 9 that a high quality weld was obtained on stainless steels by adding a small amount of hydrogen. Hydrogen is a reducing gas, and hence combines with oxygen and hinders the formation of oxide on the weld surface;<sup>11–14</sup> therefore, high quality welds with a clean surface can be obtained. Furthermore, the addition of hydrogen assists in the promotion of good puddle fluidity and wetting action on the stainless steel welds.<sup>7,13</sup> Accordingly, a smooth weld metal can be obtained using an Ar–H<sub>2</sub> mixture.

#### Effect of micro-plasma arc lengths on weld morphology

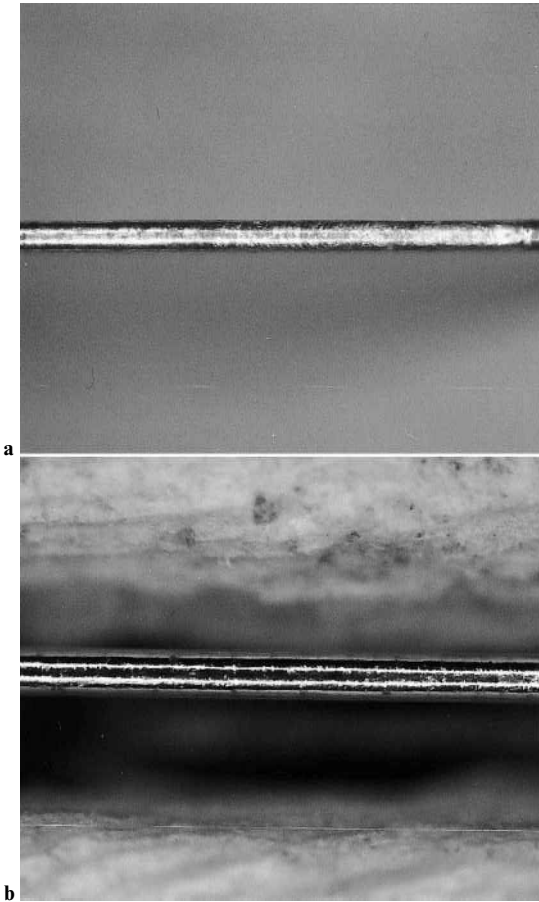
In the present work, the distance by which the electrode is recessed within the constricting nozzle was fixed at 1 mm, whereas the distance from the outer face of the constricting nozzle to the workpiece was varied. The effect of nozzle standoff distance on the geometry of the weld bead is



a pure argon (arc voltage 19.5 V); b Ar–5%H<sub>2</sub> mixture (arc voltage 21.3 V)

#### 8 Macroscopic view of edge joint welds produced using same arc current intensity of 2.5 A and welding speed of 2.0 rev min<sup>-1</sup>, but under different shielding mixtures (optical)

shown in Fig. 10. The experimental results clearly indicate a low sensitivity of puddle size to changes in nozzle standoff distance. As shown in Fig. 10, the weld depth/width ratio for a 3 A plasma arc current in an Ar–H<sub>2</sub> shielding gas varies from 0.85 to 0.81, a change of about 5%, as the nozzle standoff distance increases from 0.2 to 0.8 mm. The needle plasma arc assumes a collimated shape and, as the micro-plasma arc length is varied within normal limits, the heat transfer rate per unit area and the arc current intensity are virtually constant. Thus, a needle plasma arc can allow greater tolerance of variations in arc length.



a pure argon shielding gas; b Ar-5% $H_2$  mixture

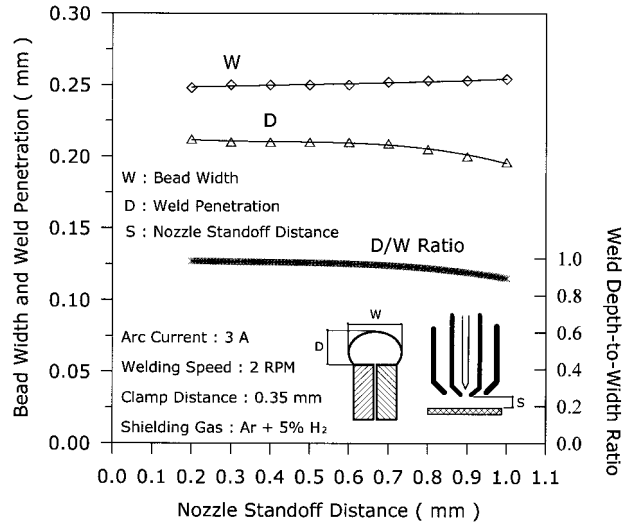
**9 Effect of hydrogen addition to argon shielding gas on weld quality in type 304 stainless steel weld metals (optical)  $\times 40$**

**Effect of process parameters on acceptable welding zone**

Figure 11 shows the influence of micro-PAW process parameters on the acceptable welding zone of the edge joint. All the welds were produced using an arc length of 1.5 mm on 0.1 mm thickness stainless steels, using an Ar-5% $H_2$  shielding gas mixture. At low arc currents, the welds were unfused because the heat input was insufficient to melt the specimens (Fig. 12a); however, at higher arc currents, smooth and uniform welds could be obtained (Fig. 12b). A further increase in the current tended to lead to formation of uneven or intermittent weld surfaces because of the excessive heat input, which results in incomplete weld profiles (Fig. 12c and d). Figure 11 indicates that an acceptable welding zone (shaded region) is formed within a particular range of arc current and welding speed at a given arc length. The bead width is proven to be proportional to the weld penetration. The quality of the weld is satisfactory if the bead width is between 2.1 and 2.6 $t$ , which corresponds to a weld penetration of 1.7 to 2.2 $t$ , where  $t$  is the thickness of the test specimen. In this acceptable welding zone, a sound weld bead geometry in an edge joint can be achieved, as shown in Fig. 13.

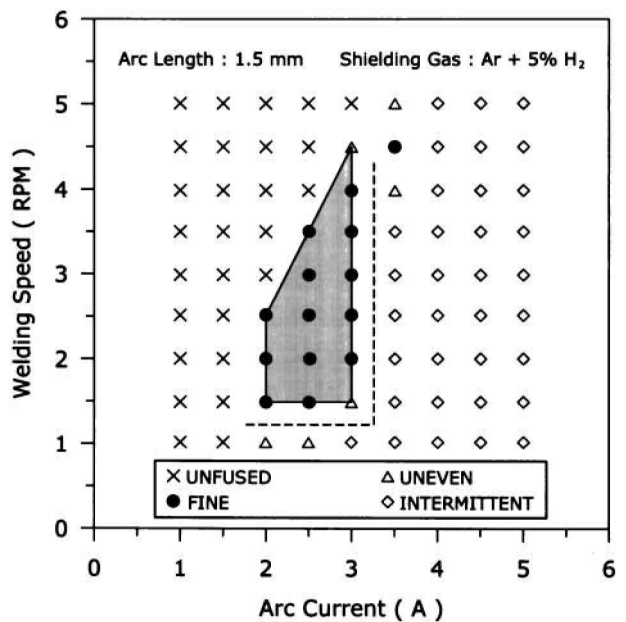
**Effect of clamp distance on weld bead geometry**

To characterise the welding process, one or more basic features that are a function of the process must be selected.

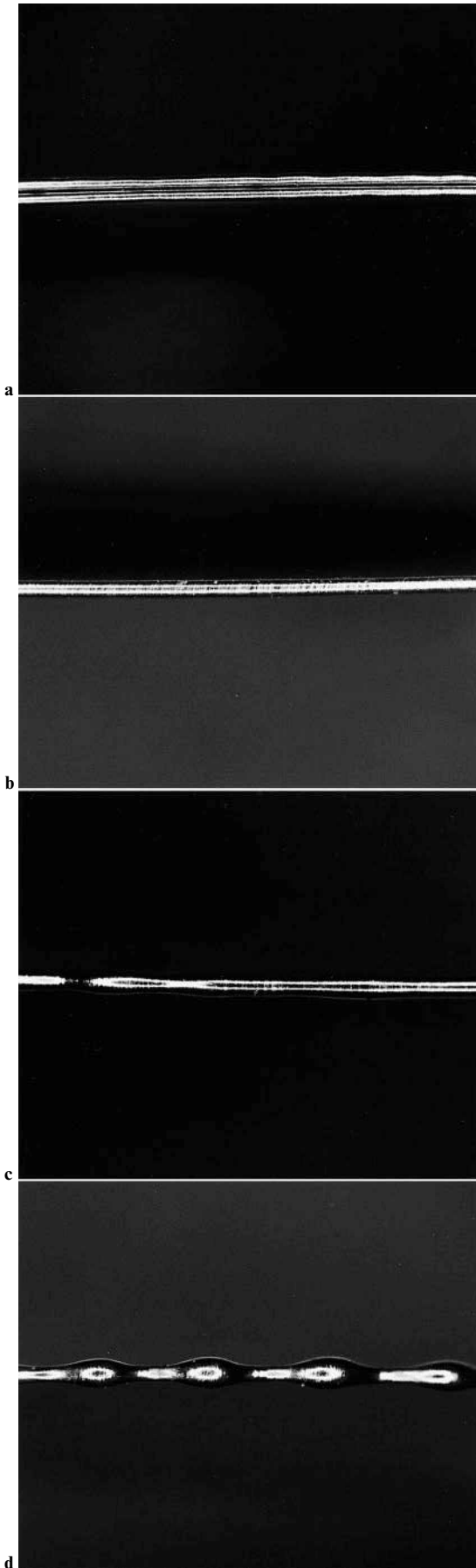


**10 Effect of nozzle standoff distance on weld bead geometry during micro-PAW process**

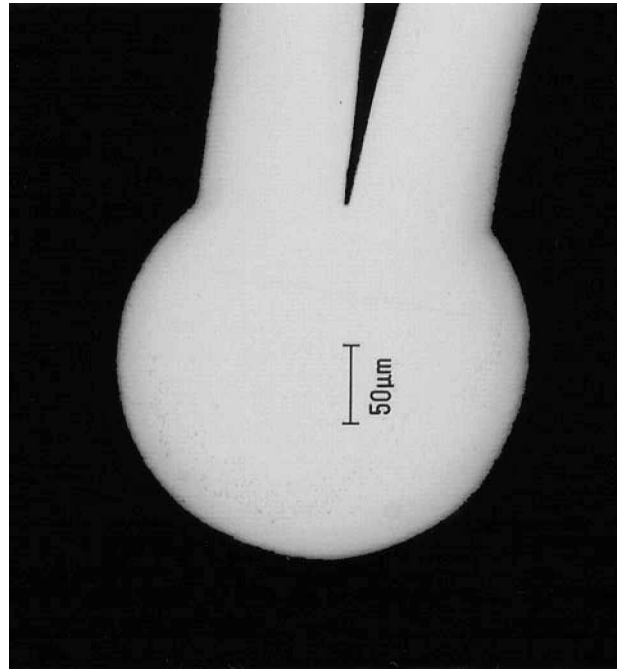
Bead width, weld penetration, and weld depth/width ratio were selected as being most useful in characterising the process. A note of caution is that the clamping design may significantly affect weld bead geometry. Figure 14 shows the effect of clamp distance on the weld bead geometry of an edge joint at constant arc current, welding speed, and plasma arc length. A greater clamp distance, allowing more free space to form a weld, tends to increase the weld depth/width ratio. When the clamp distances are below approximately 0.25 mm, the edge joint welds cannot form a circular cross-section (Fig. 15a and b). When the clamp distances are greater than 0.30 mm, roughly circular edge joint welds (width > 2 $t$ ) can be formed (Fig. 15c and d). In the present work it was found that satisfactory edge joint welds (width > 2 $t$ ) and penetration > 2 $t$ ) could be formed using a clamp distance of 0.35 mm. However, warping of the joint edges starts to



**11 Effect of process parameters of micro-PAW on acceptable welding zone for edge joint on 0.1 mm thickness stainless steels**



12 Weld configurations of *a* unfused, *b* smooth and uniform, *c* uneven, and *d* intermittent welds (optical)  $\times 25$

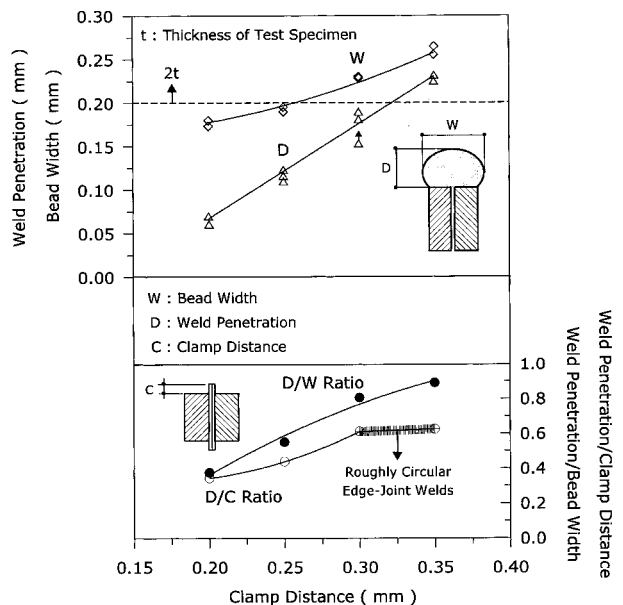


13 Macroscopic section (optical) of edge joint weld within acceptable welding zone (arc current 2.6 A, welding speed 1.5 rev min<sup>-1</sup>, plasma arc length 1.5 mm, and clamp distance 0.35 mm)

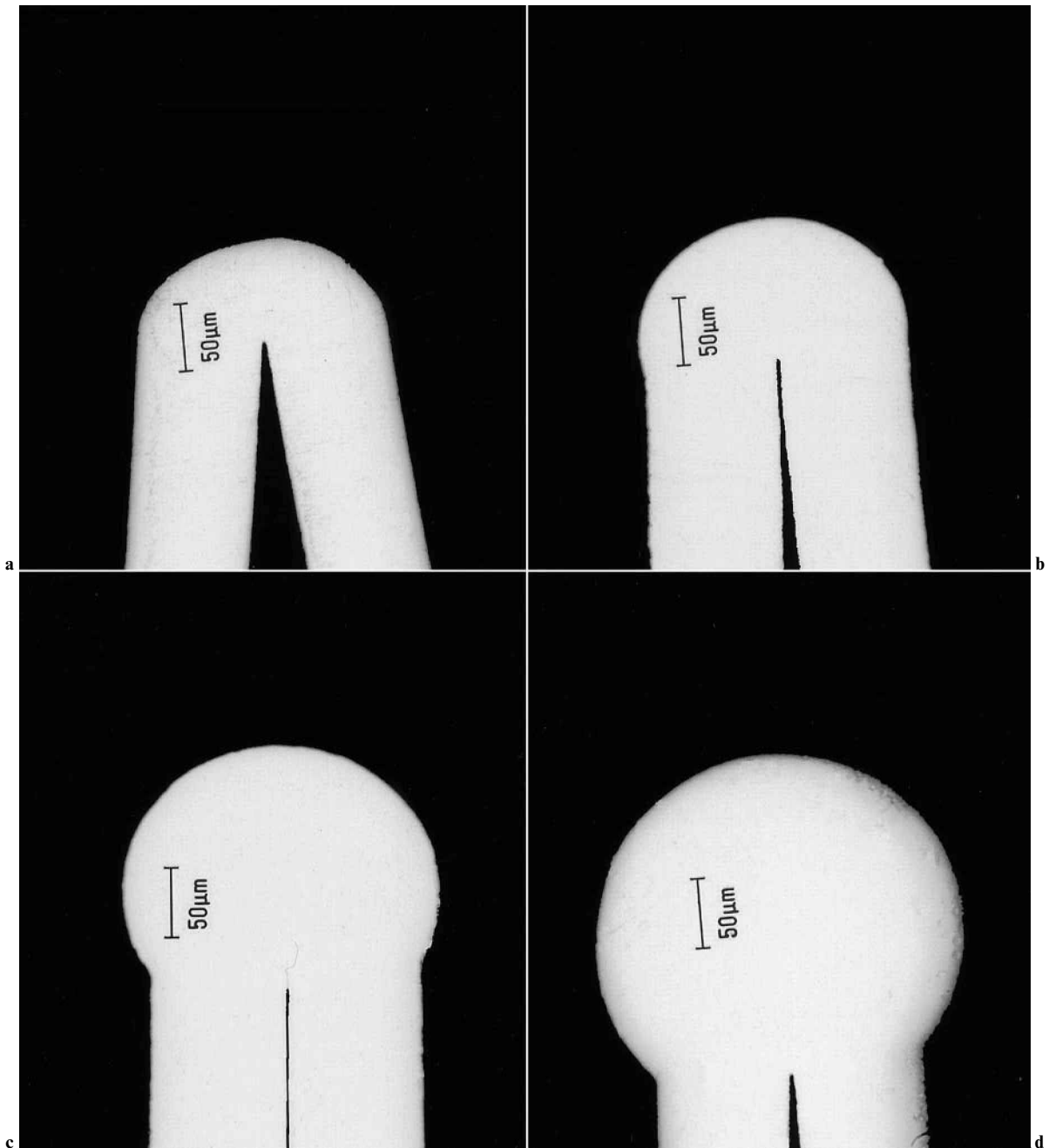
occur at clamp distances greater than 0.40 mm. Additionally, Fig. 14 also shows that using the micro-PAW technique, the roughly circular edge joint penetration produced on a 0.1 mm thickness stainless steel is about 60% of the clamp distance.

**Process application: welded bellows**

Bellows are expected to provide a hermetic seal with a low resistance to mechanical motion. They are used in vacuum systems, semiconductors, medical applications, petrochemical



14 Relationship between weld bead geometry and clamp distance



15 Macroscopic sections (optical) showing effect of clamp distance of *a* 0.20, *b* 0.25, *c* 0.30, and *d* 0.35 mm on weld bead geometry of edge joint (arc current 2.7 A, welding speed 2.2 rev min<sup>-1</sup>, and plasma arc length 1.5 mm)

applications, instrumentation industries, and other contexts. Welded bellows have been successfully manufactured using the present micro-PAW technique. A stainless steel strip having a 0.1 mm thickness wall was stamped to produce washer shaped diaphragms having concentric circular ripples (Fig. 16*a*). Pairs of diaphragms were welded along the inside edge to form 'convolutions'. These convolutions were then stacked together and their outside edges were welded. The resulting product was a welded bellows, which is a highly flexible metal tube (Fig. 16*b*). The results of the present work indicate that the 1.5 mm length, 2.8 A needle plasma produced clean, smooth, and uniform edge joint welds at a speed of 1.5 rev min<sup>-1</sup>. In these experiments, welding was performed in an Ar–5% $H_2$  mixture shielding gas.

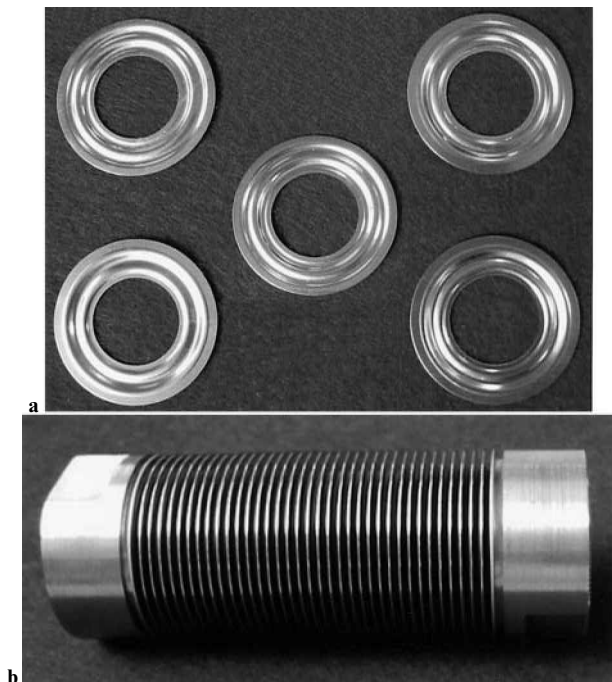
## CONCLUSIONS

1. In the low current plasma welding process, the volt–ampere characteristic curve is almost flat. Consequently, this technique can provide an arc that is stable at very low currents for welding thin metals.

2. The collimated shape of the low current plasma arc is mainly responsible for the low sensitivity of the weld morphology to variations in the nozzle standoff distances.

3. As hydrogen is added to the argon shielding gas, increasing the arc voltage and consequently the arc power, the efficiency of the heat transfer to the fusion zone increases, melting a larger quantity of base metal.

4. In PAW of stainless steel in an Ar– $H_2$  mixture, a stable process and high quality welds having very smooth surfaces can be achieved.



16 Samples of *a* diaphragms and *b* welded bellows

5. Satisfactory edge joint welds can be formed using a clamp distance of 0.35 mm, and for the present micro-plasma welding technique on 0.1 mm thickness stainless steel, the roughly circular edge joint penetration produced is about 60% of the clamp distance.

#### REFERENCES

1. S. E. BARHORST, E. H. DAGGETT, S. A. HILTON, J. T. PEROZEK and E. SPITZER: in 'Welding handbook', (ed. R. L. O'Brien), 8th edn, Vol. 2, 330–350; 1991, Miami, FL, American Welding Society.
2. S. KOU: in 'Welding metallurgy', 1st edn, 3–27; 1987, Toronto, Ont., Canada, John Wiley & Sons.
3. H. B. CARY: in 'Modern welding technology', 4th edn, 70–106; 1998, Englewood Cliffs, NJ, Prentice-Hall.
4. W. LUCAS: in 'TIG and plasma welding', 1st edn, 80–108; 1990, Cambridge, UK, Abington Publishing.
5. C. D. LUNDIN and W. J. RUPRECHT: *Weld. J.*, 1974, **53**, (1), 11–19.
6. Y. M. ZHANG and S. B. ZHANG: *Weld. J.*, 1999, **78**, (2), 53s–58s.
7. E. F. GORMAN: *Weld. J.*, 1969, **48**, (7), 547–556.
8. R. L. O'BRIEN: *Weld. Res. Counc. Bull.*, 1968, **131**, 1–37.
9. J. F. LANCASTER: in 'The physics of welding', 2nd edn, 146–227; 1986, Oxford, UK, Pergamon Press.
10. C. M. CHO, H. C. CHIANG and C. N. DONG: Proc. 1st National Conf. on 'Welding technology', Taipei, Taiwan, December 1987, Welding Assoc. of the Republic of China, 159–172.
11. W. LUCAS: *Weld. Met. Fabr.*, June 1992, **60**, 218–225.
12. B. BENNETT: *Weld. Met. Fabr.*, July 1990, **58**, 335–336.
13. D. HILTON: *Weld. Met. Fabr.*, July 1990, **58**, 332–334.
14. M. ONSØIEN, R. PETERS, D. L. OLSON and S. LIU: *Weld. J.*, 1995, **74**, (1), 10s–15s.